nature medicine

Cardiomyocyte-restricted peroxisome proliferator-activated receptor-δ deletion perturbs myocardial fatty acid oxidation and leads to cardiomyopathy

Lihong Cheng[1], Guoliang Ding[1], Qianhong Qin[1], Yao Huang[1], William Lewis[2], Nu He[3], Ronald M Evans[4], Michael D Schneider[5], Florence A Brako[1], Yan Xiao[1], Yuqing E Chen[1] & Qinglin Yang[1]

Fatty acid oxidation (FAO) is a primary energy source for meeting the heart's energy requirements[1–3]. Peroxisome proliferator-activated receptor-δ (PPAR-δ) may have important roles in FAO[4–8]. But it remains unclear whether PPAR-δ is required for maintaining basal myocardial FAO. We show that cre-loxP-mediated cardiomyocyte-restricted deletion of PPAR-δ in mice downregulates constitutive expression of key FAO genes and decreases basal myocardial FAO. These mice have cardiac dysfunction, progressive myocardial lipid accumulation, cardiac hypertrophy and congestive heart failure with reduced survival. Thus, chronic myocardial PPAR-δ deficiency leads to lipotoxic cardiomyopathy. Together, our data show that PPAR-δ is a crucial determinant of constitutive myocardial FAO and is necessary to maintain energy balance and normal cardiac function. We suggest that PPAR-δ is a potential therapeutic target in treating lipotoxic cardiomyopathy and other heart diseases.

PPAR-δ knockout leads to embryonic lethality and growth retardation in surviving mice[9,10]. To avoid these global defects, we used a *cre-lox*P-mediated cardiomyocyte-restricted gene targeting approach by crossing mice carrying a *loxP*-flanked allele of *Ppard* (*Ppard*$^{flox/flox}$), the gene that encodes PPAR-δ (ref. 9), with cardiomyocyte-restricted Cre-expressing (α-MyHC-Cre) mice[11,12] to study the role of PPAR-δ in the heart *in vivo* (see **Supplementary Fig. 1** online). Using samples from homozygous hearts, we confirmed at transcript and protein levels that mice contained the cardiomyocyte-restricted knockout of *Ppard* (CR-*Ppard*$^{-/-}$) (**Fig. 1a,b**). PPAR-δ expression was unchanged in other tissues, including skeletal muscle, liver, lung and fat (data not shown). In addition, no substantial difference could be detected in transcript abundance of PPAR-α and -γ in the hearts of 2- and 9-month-old CR-*Ppard*$^{-/-}$ mice compared to those of control mice (**Supplementary Fig. 2** online). Thus, any molecular, biochemical or pathophysiological changes shown in the hearts of CR-*Ppard*$^{-/-}$ mice should be due to the cardiomyocyte-restricted PPAR-δ deletion.

We examined transcript levels of mitochondrial and peroxisomal FAO genes. Muscle carnitine palmitoyl transferase-1 (mCPT-1), 3-oxoacyl-CoA thiolase (thiolase), uncoupling protein 3 (UCP3), long-chain acyl-CoA dehydrogenase (LCAD), malonyl-CoA decarboxylase (MCD), pyruvate dehydrogenase kinase 4 (PDK4), very long-chain acyl-CoA dehydrogenase (VLCAD) and acyl-CoA oxidase 1 (ACOX1) were considerably downregulated in the hearts of CR-*Ppard*$^{-/-}$ mice as compared to α-MyHC-Cre and *Ppard*$^{flox/flox}$ mice. The transcript levels were decreased by 43% for mCPT-I; 38.8% for thiolase, 50% for UCP3, 48.7% for LCAD, 32.7% for MCD, 66.2% for PDK4, 25.6% for VLCAD and 51.4% for ACOX1 compared to controls, respectively (**Fig. 1c**). Protein levels of mCPT-I and UCP3 were decreased correspondingly (**Fig. 1d**). As expected, we observed a considerable reduction in the rate of palmitic acid oxidation in 2-month-old PPAR-δ-deficient left ventricles compared to that from controls (**Fig. 1e**), but we observed an upregulation in glucose uptake in cardiomyocytes in 2-month-old PPAR-δ-deficient cardiomyocytes (**Fig. 1f**). These results indicate that decreased cardiac FAO gene transcripts resulting from PPAR-δ deficiency are responsible for reduced basal FAO. Notably, conventional *Ppara* knockout mice also show decreased expression of myocardial FAO genes[13]. However, PPAR-α-null mice require fasting to elicit a robust phenotype[14]. We showed previously that a PPAR-δ-selective ligand can restore FAO gene expression in cultured cardiomyocytes from PPAR-α knockout mice[8]. Using a similar approach, we treated cultured cardiomyocytes from the hearts of 3-month-old CR-*Ppard*$^{-/-}$ and control mice with PPAR-α- and PPAR-δ-selective ligands: Wy14643 and GW0742, respectively. Decreased transcript levels of mCPT-1, thiolase, PDK4 and ACOX1 in cardiomyocytes of CR-*Ppard*$^{-/-}$ mice were restored by the treatment with Wy14643 but not with GW0742, whereas transcripts of these genes increased considerably with both Wy14643 and GW0742 treatment in control cardiomyocytes (**Fig. 1g**).

[1]Cardiovascular Research Institute, Morehouse School of Medicine, Atlanta, Georgia 30310, USA. [2]Department of Pathology and Laboratory Medicine, Emory University, Atlanta, Georgia 30322, USA. [3]Department of Pharmacology, Morehouse School of Medicine, Atlanta, Georgia 30310, USA. [4]Howard Hughes Medical Institute, The Salk Institute for Biological Studies, La Jolla, California 92037, USA. [5]Center for Cardiovascular Development, Baylor College of Medicine, Houston, Texas 77030, USA. Correspondence should be addressed to Q.Y. (qyang@msm.edu).

Published online 10 October 2004; doi: 10.1038/nm1116

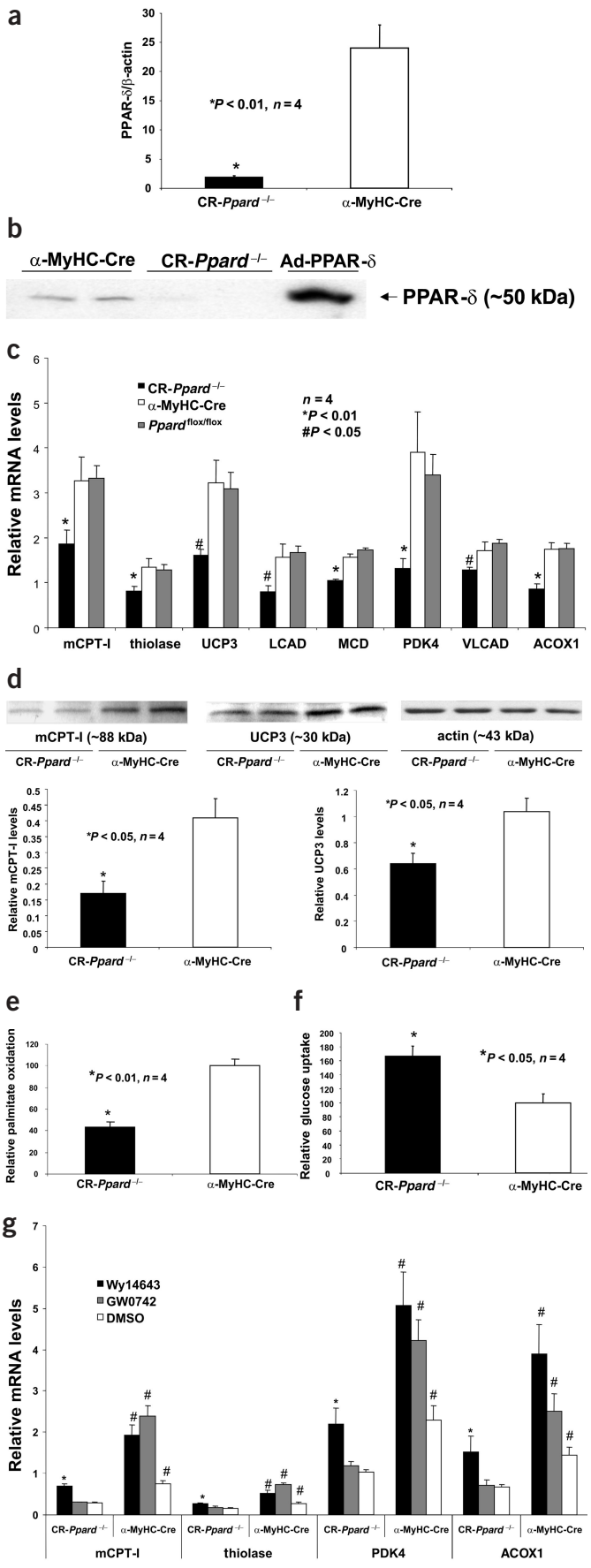

We further investigated whether the reduced basal myocardial FAO rate in CR-*Ppard*$^{-/-}$ hearts results in a changed lipid profile and in histopathology. Myocardial triglyceride levels increased slightly by 10 weeks of age and were almost doubled in surviving CR-*Ppard*$^{-/-}$ mice at 9 months of age provided with *ad libitum* rodent chow (**Fig. 2a**). Consistent with this biochemical finding, neutral lipid (determined histologically with oil red O staining) was markedly increased in sections from the hearts of adult (5–9 month-old) but not young (2-month-old) CR-*Ppard*$^{-/-}$ mice compared to those of controls (**Fig. 2b**). CR-*Ppard*$^{-/-}$ mouse hearts showed progressively increased myocardial triglyceride content and neutral lipid droplets histopathologically with age in the absence of stress or dietary manipulation. Because expression of other PPAR subtypes was unchanged by age (**Supplementary Fig. 2** online), it is reasonable to suggest that changes in FAO gene expression and FAO rates in PPAR-δ-deficient hearts are causally related to PPAR-δ deficiency in cardiomyocytes. Furthermore, decreased tissue FAO may result in repressed lipogenesis to compensate for reduced FAO[15]. Whereas protein levels of the PPAR-γ coactivator-1α (PGC-1α) (**Supplementary Fig. 3** online) and acyl-CoA carboxylase (ACC) (**Fig. 2c**) were unchanged, the level of phosphorylated ACC (pACC) in the hearts of CR-*Ppard*$^{-/-}$ mice was significantly increased ($P < 0.05$) compared to that of control hearts (**Fig. 2c**). Along with the increased pACC level, we observed a concomitant upregulation of AMP-dependent kinase (AMPK) activity (**Fig. 2d**). As a result, myocardial malonyl CoA content was about 40% lower in CR-*Ppard*$^{-/-}$ than in control mice (**Fig. 2e**). These data indicate that lipogenesis is repressed in response to increased myocardial fatty acids. However, the repression of lipogenesis in CR-*Ppard*$^{-/-}$ mouse hearts seems insufficient to rescue the loss of basal myocardial FAO.

Although no overt pathological phenotype was observed in CR-*Ppard*$^{-/-}$ mice before adulthood, cardiac hypertrophy was evident in adult CR-*Ppard*$^{-/-}$ mice. Except in mice with signs of heart failure, we did not detect any difference in body weight. Normalized cardiac mass (determined by the ratio of heart weight to body weight) was significantly greater ($P < 0.01$) in CR-*Ppard*$^{-/-}$ mice at 4 months of age (**Fig. 3a**), but not at 2 months of age (**Fig. 3a**). Ventricular expression of molecular markers of cardiac hypertrophy, namely atrial natriuretic factor (ANF), brain natriuretic protein (BNP) and skeletal α-actin, were about 10-, 14- and 4-fold higher, respectively, than in controls (**Fig. 3b**). As early as 4 months of age, some CR-*Ppard*$^{-/-}$ mice developed dilated cardiomyopathy resembling end-stage heart failure, characterized by enlarged

Figure 1 PPAR-δ and FAO gene expression, palmitate oxidation and glucose uptake rates. (**a**) Real-time RT-PCR results of PPAR-δ transcript levels in α-MyHC-Cre and CR-*Ppard*$^{-/-}$ hearts are shown. (**b**) Western blot analysis of PPAR-δ on nuclear protein samples extracted from isolated adult cardiomyocytes of CR-*Ppard*$^{-/-}$ and α-MyHC-Cre mice. Ad-PPARδ is a positive control for specificity of antibody to PPAR-δ. (**c**) Transcript levels of genes encoding key FAO enzymes from left ventricle of 2-month-old CR-*Ppard*$^{-/-}$, α-MyHC-Cre and *Ppard*$^{flox/flox}$ mice. Data are expressed as mean ± s.e.m. (**d**) Western blot analyses of mCPT-I and UCP3 in CR-*Ppard*$^{-/-}$ and α-MyHC-Cre hearts. (**e**) Relative rate of [^{14}C]palmitate oxidation in left ventricular tissues from 2-month-old CR-*Ppard*$^{-/-}$ and α-MyHC-Cre hearts. (**f**) Relative level of glucose uptake in cultured cardiomyocytes isolated from left ventricles of 2-month-old CR-*Ppard*$^{-/-}$ and α-MyHC-Cre hearts. (**g**) FAO gene expression in cultured cardiomyocytes with Wy14643 and GW0742 treatment. *$P < 0.05$: Wy14643 or GW0742 versus DMSO-treated CR-*Ppard*$^{-/-}$ cardiomyocytes; #$P < 0.05$: CR-*Ppard*$^{-/-}$ versus α-MyHC-Cre cardiomyocytes with same treatment.

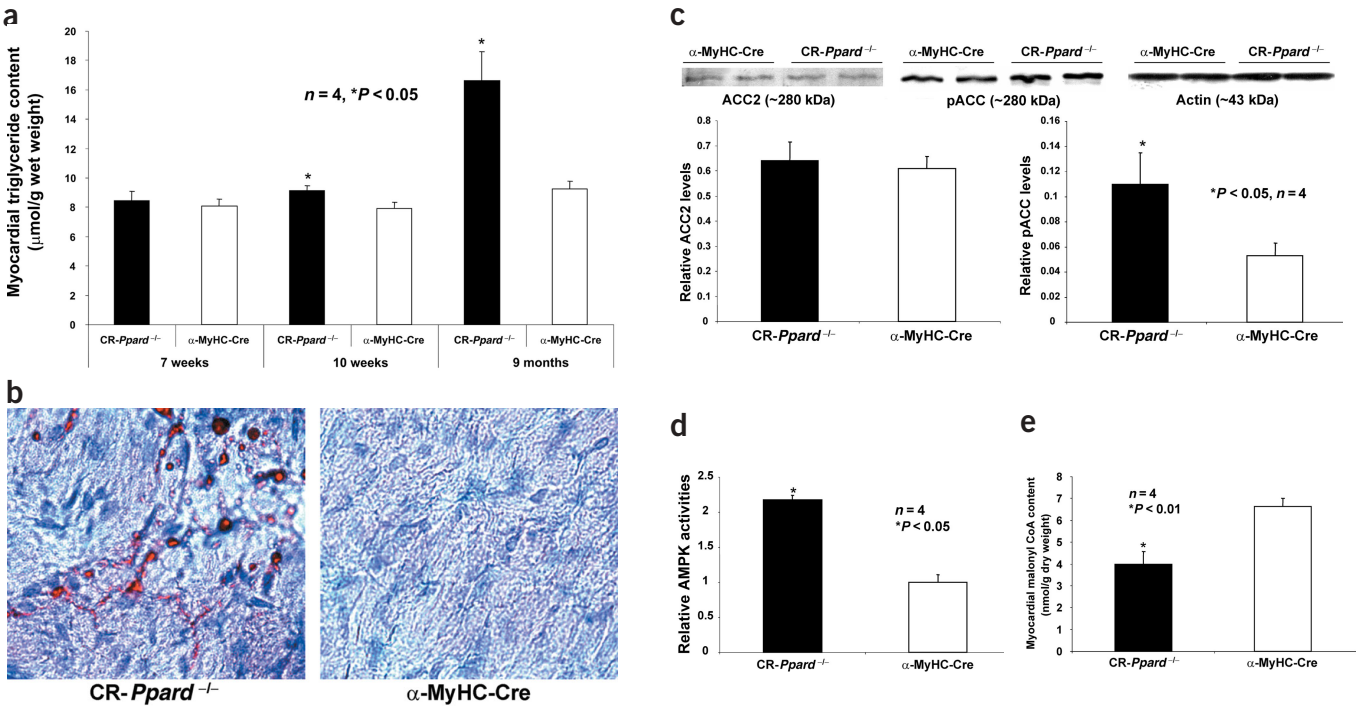

Figure 2 Myocardial lipid accumulation and lipogenesis. (**a**) Myocardial triglyceride content in hearts from CR-*Ppard*$^{-/-}$ and α-MyHC-Cre mice at 7 weeks, 10 weeks and 9 months of age. (**b**) Representative photomicrographs depicting the histologic appearance of ventricular tissue from 8-month-old CR-*Ppard*$^{-/-}$ and α-MyHC-Cre mice (image at ×400, oil red O). (**c**) Relative protein levels of ACC and pACC from samples of 5-month-old CR-*Ppard*$^{-/-}$ and α-MyHC-Cre hearts. (**d**) Relative AMPK activities in left ventricle samples of 5-month-old CR-*Ppard*$^{-/-}$ and α-MyHC-Cre hearts. (**e**) Myocardial malonyl-CoA levels in 5-month-old CR-*Ppard*$^{-/-}$ and α-MyHC-Cre hearts.

hearts, subcutaneous edema, tachypnea and pleural effusions. Heart weights normalized to tibial lengths were considerably greater in CR-*Ppard*$^{-/-}$ mice that died from heart failure than in age- and gender-matched controls (**Supplementary Fig. 4** online). Images of representative mice and their hearts from CR-*Ppard*$^{-/-}$ and controls at 9 months of age are shown in **Figure 3c**. We observed enlargement and severe dilation of the hearts of CR-*Ppard*$^{-/-}$ mice, which had a very thin ventricular wall. Sections of hearts from CR-*Ppard*$^{-/-}$ mice stained with Masson's trichrome showed markedly increased interstitial fibrosis and hypertrophied cardiomyocytes (**Fig. 3c**). Because cellular lipid accumulation triggers programmed cell death in cardiac and other tissues[16–21], we examined ventricular tissues for evidence of apoptosis with TUNEL assays in mice at various ages preceding congestive heart failure. In CR-*Ppard*$^{-/-}$ mice, in hearts that showed neutral lipid accumulation but absence of dilated cardiomyopathy, we found approximately 1 in 10^5 to 1 in 10^4 positively staining cardiomyocytes (**Fig. 3d**). We did not observe positive staining in the hearts of CR-*Ppard*$^{-/-}$ mice before 2 months of age and in control mice up to 10 months of age. Cytochrome *c* levels in the cytosolic fraction of extracts from the hearts of CR-*Ppard*$^{-/-}$ mice increased markedly (**Fig. 3e**). We assessed ultrastructural features of cardiomyocytes from CR-*Ppard*$^{-/-}$ mice at various ages. Neutral lipid droplets were abundant in sections from the hearts of 8-month-old (**Fig. 3f**) but not 6–8 week-old (data not shown) CR-*Ppard*$^{-/-}$ mice. We also found degenerating cardiomyocytes with disrupted sarcomeric architecture (**Fig. 3f**). Mitochondria of CR-*Ppard*$^{-/-}$ cardiomyocytes contained numerous dense electron bodies (**Fig. 3f**). Peroxisomes in the CR-*Ppard*$^{-/-}$ hearts appeared as enlarged membrane-enclosed structures containing lipid and matrix-type materials (**Fig. 3f**). In longevity studies, we observed that mice died at 4–10 months of age, independent of gender. Expression of key FAO genes remained low in CR-*Ppard*$^{-/-}$ mice with cardiac hypertrophy and heart failure (**Supplementary Fig. 5** online). Kaplan-Meier survival of CR-*Ppard*$^{-/-}$ mice was substantially reduced compared to that of controls (**Fig. 3g**). We did not detect overt cardiac pathological differences in α-MyHC-Cre and *Ppard*$^{flox/flox}$ mice over their lifetime compared with nontransgenic mice.

Because myocardial energetic disturbances were present in the hearts of CR-*Ppard*$^{-/-}$ mice, we assessed cardiac performance in hearts from 6- to 8-week-old mice preceding myocardial lipid accumulation and cardiac hypertrophy. Rates of cardiac contractility and relaxation, indicated by maximal and minimal dP/dt, respectively, were reduced 11% and 13% in CR-*Ppard*$^{-/-}$ mouse hearts compared to control hearts (**Fig. 4a**,**b**). Although heart rates were similar, left ventricular end-diastolic pressure (LVEDP) and 90% relaxation time (RT90) were significantly greater in the hearts of CR-*Ppard*$^{-/-}$ mice than in those of the controls (**Fig. 4c**,**d**), indicating impaired diastolic function in CR-*Ppard*$^{-/-}$ mice. Consequently, we observed left ventricular developed pressure (LVDP) and cardiac output depression in CR-*Ppard*$^{-/-}$ mice compared to control mice (**Fig. 4e**,**f**). These results indicate that PPAR-δ is essential for maintaining basal cardiac function, possibly through maintenance of basal myocardial FAO. A decline in cardiac function may initiate cardiac pathological changes; progressive myocardial lipid accumulation should greatly exacerbate pathological changes in older CR-*Ppard*$^{-/-}$ mice.

The striking cardiac pathological development in CR-*Ppard*$^{-/-}$ mice characterized by cardiac dysfunction, myocardial lipid accu-

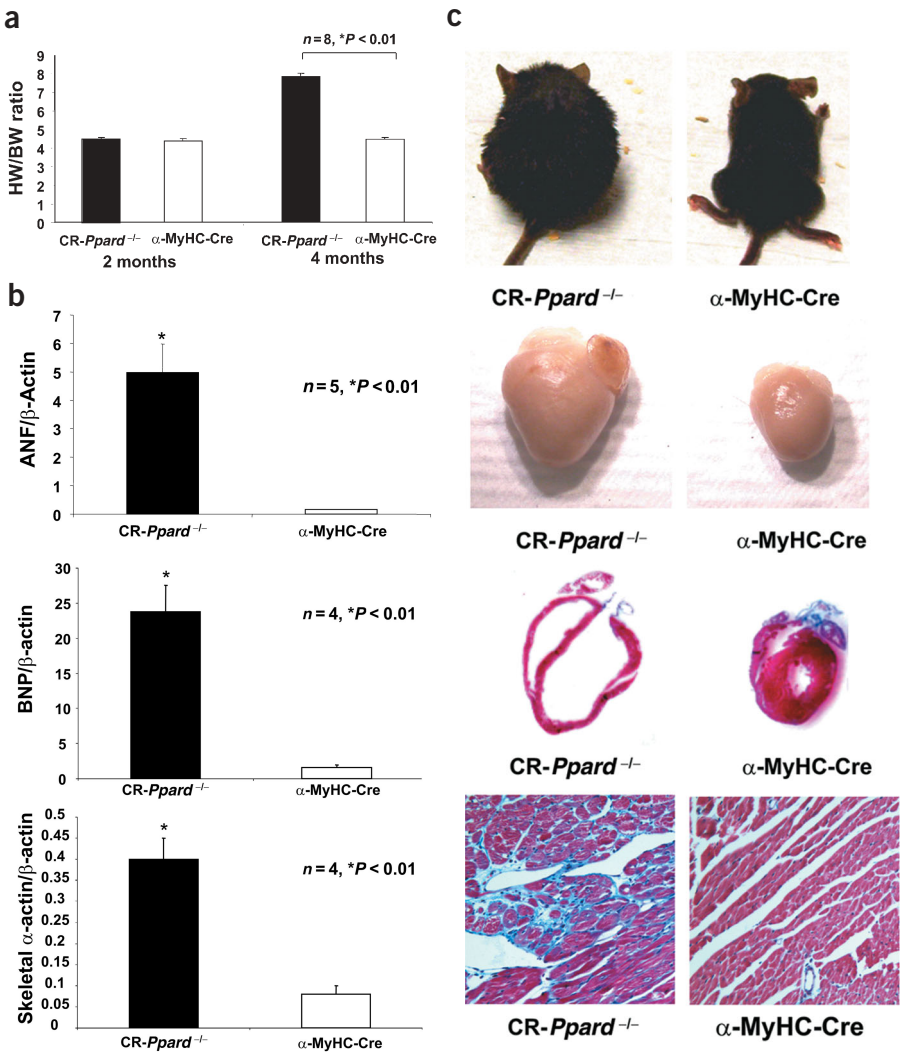

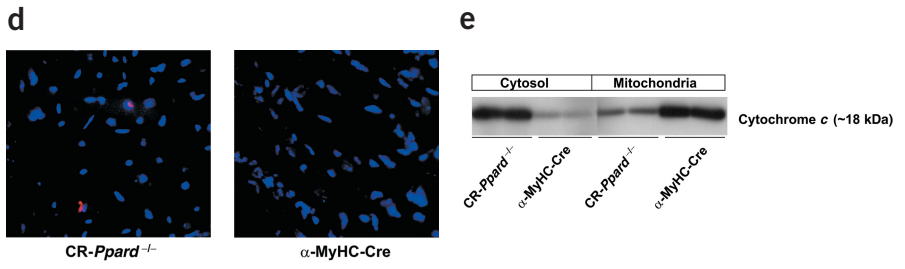

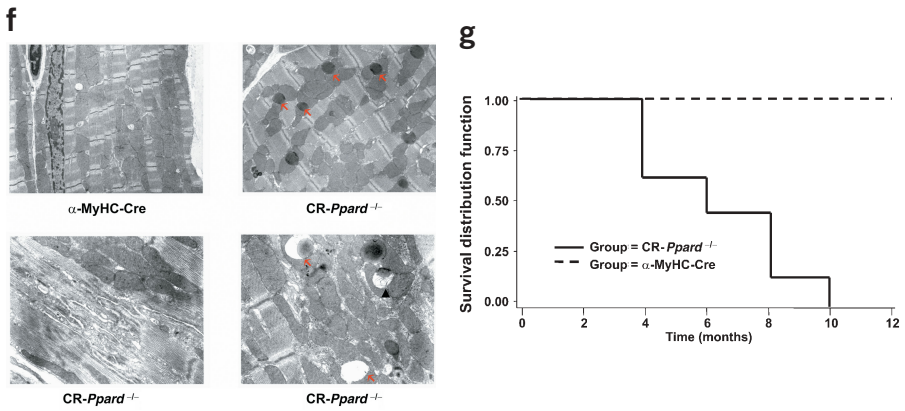

Figure 3 Cardiac hypertrophy and dilated cardiomyopathy in hearts from adult CR-*Ppard*$^{-/-}$ mice. (**a**) Ratios of heart weight to body weight (HW/BW) in 2-month-old and 4-month-old CR-*Ppard*$^{-/-}$ and α-MyHC-Cre mice. (**b**) mRNA abundance of ANF, BNP and skeletal α-actin (molecular markers of left ventricle hypertrophy) in samples from hearts of 4-month-old CR-*Ppard*$^{-/-}$ and α-MyHC-Cre mice. (**c**) Representative photographs of a moribund CR-*Ppard*$^{-/-}$ mouse and a healthy α-MyHC-Cre mouse and their respective hearts at 9 months of age. Heart sections and histological images (images at ×200, Masson's trichrome) of hearts from a CR-*Ppard*$^{-/-}$ mouse and a α-MyHC-Cre littermate at 9 months of age. (**d**) Representative image of apoptotic cardiomyocytes in a section of a heart of a 5-month-old CR-*Ppard*$^{-/-}$ mouse (images at ×400). Red staining indicates apoptotic cells; blue indicates nuclei. (**e**) Western blots of cytochrome *c* in mitochondrial and cytosolic fractions in extracts from hearts of 5-month-old CR-*Ppard*$^{-/-}$ and α-MyHC-Cre mice. (**f**) TEM examination of the myocardial ultrastructure of an 8-month-old α-MyHC-Cre mouse and an 8-month-old CR-*Ppard*$^{-/-}$ mouse, as indicated. Upper right; arrows indicate lipid droplets. Degenerating cardiomyocytes had a damaged sarcomeric structure and mitochondria with numerous electron-dense bodies (lower left). Large lipid droplets (arrows) and an enlarged peroxisome with membrane-bound structure containing lipid and remnant matrix-type materials (arrow head) (lower right). Upper panels: images at ×15,000; lower panels: images at ×36,000). (**g**) Kaplan-Meier survival curves for CR-*Ppard*$^{-/-}$ and α-MyHC-Cre mice. The survival curves are statistically different ($P < 0.001$) by log-rank test.

mulation and lipoapoptosis in the absence of fasting, high-fat diet or other pathological stresses strongly supports a crucial role for PPAR-δ in maintaining normal FAO in the heart and cardiac function. Results from this study thus provide important insights into the biological roles of PPAR-δ in cardiac pathophysiology and hence provide new therapeutic targets for the treatment of heart disease.

METHODS

Animals. Animals received food and water *ad libitum*, and lighting was maintained on a 12-h cycle. All experimental procedures were conducted in accordance with the Guide for Care and Use of Laboratory Animals of the National Institutes of Health, and were approved by the Institutional Animal Care and Use Committee of Atlanta University Center. (For the generation and genotyping of the CR-*Ppard*$^{-/-}$ mice, see **Supplementary Methods** online).

Transcript analyses. We extracted total RNA samples using an RNA extraction kit (Qiagen). We performed quantitative real-time RT-PCR

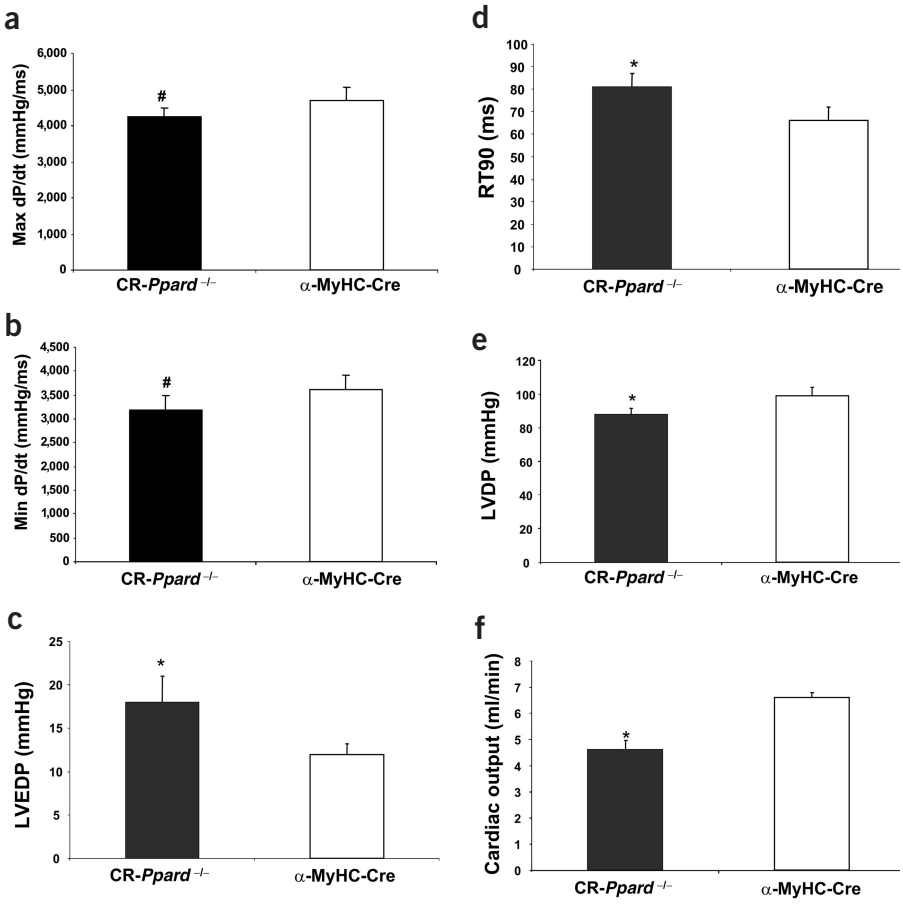

Figure 4 Isolated working heart function in CR-*Ppard*$^{-/-}$ and α-MyHC-Cre mice. Cardiac performance was evaluated among hearts from 6–8-week-old CR-PPAR-δ$^{-/-}$ and α-MyHC-Cre mice. (**a**,**b**) Maximal and minimal dP/dt values, indicating rates of cardiac contractility and relaxation, respectively, are shown. (**c**–**f**) Values of left ventricular end-diastolic pressure (LVEDP), 90% relaxation time (RT90), left ventricular developed pressure (LVDP) and cardiac output are shown, respectively. Values are presented as mean ± s.d. $n = 7$, $^{\#}P < 0.05$ and $^{*}P < 0.01$.

analyses (Roche LightCycler PCR system) to determine transcript levels of target genes.

Protein analysis. We extracted nuclear and cytosolic proteins using a nuclear protein extraction kit (Pierce). Mitochondria were extracted using a kit from Sigma. We subjected samples to SDS-PAGE gels and performed immunoblotting. We obtained antibodies from commercial sources: PPAR-δ, pan-actin, PGC-1α and cytochrome *c* from Santa Cruz Biotechnology; ACC and pACC from Upstate Biotechnology; and mCPT-1 and UCP3 from Alpha Diagnostic International. Protein samples from cardiomyocytes transduced with an adenoviral PPAR-δ construct were used as positive control for antibodies to PPAR-δ.

Myocardial triglyceride content. Myocardial triglyceride content was assayed as described previously[22]. Briefly, left ventricular tissues were homogenized with ice-cold chloroform/methanol/ water mixture (2:1:0.8) for 2 min. We added additional chloroform and water to separate the organic and aqueous layers. After centrifugation, we removed the aqueous layer, decanted the chloroform layer and evaporated the mixture at 70 oC. We dissolved the residue in 0.5 ml of isopropanol, and assayed triglycerides with a triglyceride measurement kit from Sigma.

[1-^{14}C]Palmitate oxidation assay. We evaluated rates of FAO in heart tissue by a published palmitate oxidation assay[23] with modification. We minced left ventricles into fine pieces and preincubated them in assay buffer containing (in mM), HEPES (20), NaH_2PO_4 (1), $MgSO_4$ (0.4), $CaCl_2$ (1), NaCl (120), KCl (5), BSA (0.3), glucose (5), palmitic acid (0.05), oleic acid (0.05), pH 7.4, for 30 min at 37 °C. We added [1-^{14}C]palmitic acid (0.002 mCi and 0.004 mCi, PerkinElmer Life Sciences) and incubated the tissues an additional 30 min. We assessed the CO_2-trapping medium (NaOH, 0.1 M) for ^{14}C activity by liquid scintillation counting normalized to the weight of the tested ventricle tissues. The relative levels of [^{14}C]palmitate oxidation in CR-*Ppard*$^{-/-}$ hearts were expressed as percentage changes compared with controls (α-MyHC-Cre), which we arbitrarily set at 100%.

Adult mouse cardiomyocyte isolation and culture. We isolated adult mouse cardiomyocytes from the hearts of adult mice and cultured them as previously described[8]. We applied PPAR-α- and PPAR-δ-selective ligands, Wy14643 (10 μM) and GW0742 (10 nM), respectively, after 24 h serum-free medium culture and collected cardiomyocytes 24 h later.

Glucose uptake in isolated cardiomyocytes. We performed glucose transport assays in triplicate in 12-well (22 mm in diameter) laminin-coated tissue culture plates. We washed laminin-plated cardiomyocytes from 2-month-old mice twice with 1 ml of glucose-free DMEM, then added 1 ml of glucose-free DMEM (37 °C) containing 0–1 nM insulin, 1 mM pyruvate and 0.1% BSA. After 40 min, we added 10 μl of a 2-deoxyglucose mix containing 130 μl of glucose-free DMEM, 15 μl of 100-mM 2-deoxyglucose solution, and 5 μl of 1-μCi/μl [^{3}H]2-deoxyglucose (NEN Life Science). After 30 min, we lysed the cultured cardiomyocytes in 500 μl of NaOH (1 M) for 20 min at 37 °C. We counted a 400-μl aliquot of lysed cells to determine the specific activity of [^{3}H]2-deoxyglucose normalized to protein concentration. Specific activities of [^{3}H]2-deoxyglucose of CR-*Ppard*$^{-/-}$ were expressed as percentage changes compared with control (α-MyHC-Cre), which was arbitrarily set at 100%.

Myocardial malonyl CoA content. We extracted malonyl-CoA from freeze-dried left ventricles with 5% sulfosalicylic acid containing 50 μM of dithioerythritol in 1:9 wt/vol (mg/μl) proportion and measured them by high-performance liquid chromatography separation using previously described methodology[24,25].

AMPK activities. We measured AMPK activity using a SAMS peptide (HMRSAMSGLHLVKRR) phosphorylation assay as previously described[26]. We performed the assay in a total volume of 25 μl in the presence of 5 mM $MgCl_2$, 0.2 mM ATP, 0.2 mM AMP, 0.2 mM SAMS, 0.8 mM DTT and [γ-^{32}P]ATP for 10 min at 30 °C. At the end of incubation, we spotted 20-μl aliquots of supernatant from the reaction mixture on Whatman filter paper (P81). We washed the filter papers with cold 150 mM phosphoric acid for 40 min and with acetone for 20 min and then allowed them to dry before scintillation counting. AMPK activity of CR-*Ppard*$^{-/-}$ was expressed as fold change compared with control (α-MyHC-Cre), which was arbitrarily set at 1.

***In situ* cell death detection (TUNEL assay).** We identified apoptotic cardiomyocytes by staining on frozen heart sections using the *in situ* cell death detection kit (Roche). We also stained heart sections with DAPI to identified nuclei (blue). We identified the apoptotic cardiomyocytes with red

color nuclear staining with the presence of striations under phase-contrast view.

Pathological examinations. We stained 5-μm paraffin-embedded sections with Masson's trichrome. To detect neutral lipid, we stained frozen sections with oil red O and counterstained them with hematoxylin. We used left ventricles from fixed heart tissues for transmission electron microscope (TEM) examinations.

Kaplan-Meier survival curves. The number of mice used to calculate the survival curve included a total of 35 CR-*Ppard*$^{-/-}$ and 20 α-MyHC-Cre animals up to 11 months of age. Mice killed for experimental purposes were excluded. We analyzed the survival curves using the log-rank test.

Isolated working heart preparation. Isolated working heart function was assessed with an isolated working mouse heart apparatus from Harvard Apparatus. A 1.4-F pressure/volume catheter (Millar Instrument) was used to obtain pressure and volume values. The acquired data were subsequently accessed with the HES software from the manufacturer (Harvard Apparatus). (For detailed methodology, see **Supplementary Methods** online.)

Statistical analyses. We analyzed all data using one-factor or mixed, two-factor analysis of variance (ANOVA) using Statview 4.01 software (Abacus Concepts). Unless indicated in figure legends, values of quantitative results were expressed as mean ± s.e.m. Differences between groups and treatments were regarded as significant at the $P < 0.05$ probability level.

Note: Supplementary information is available on the Nature Medicine website.

ACKNOWLEDGMENTS

We thank J. Chatham and G.H. Gibbons for reading of the manuscript. This work was partially supported by a starting grant from Morehouse Cardiovascular Research Institute (Enhancement of Cardiovascular and Related Research Areas, NIH/NHLBI 5 UH1 HL03676-02), grants from the US National Institutes of Health (MBRS S06GM08248 and G12-RR03034) and a scientist development award from the American Heart Association national center.

COMPETING INTERESTS STATEMENT

The authors declare that they have no competing financial interests.

Received 6 April; accepted 30 August 2004
Published online at http://www.nature.com/naturemedicine

1. van der Vusse, G.J., Glatz, J.F., Stam, H.C. & Reneman, R.S. Fatty acid homeostasis in the normoxic and ischemic heart. *Physiol. Rev.* **72**, 881–940 (1992).
2. Vary, T.C., Reibel, D.K. & Neely, J.R. Control of energy metabolism of heart muscle. *Annu. Rev. Physiol.* **43**, 419–430 (1981).
3. Neely, J.R., Rovetto, M.J. & Oram, J.F. Myocardial utilization of carbohydrate and lipids. *Prog. Cardiovasc. Dis.* **15**, 289–329 (1972).
4. Wang, Y.X. *et al.* Peroxisome proliferator activated receptor δ activates fat metabolism to prevent obesity. *Cell* **113**, 159–170 (2003).
5. Tanaka, T. *et al.* Activation of peroxisome proliferator-activated receptor δ induces fatty acid β-oxidation in skeletal muscle and attenuates metabolic syndrome. *Proc. Natl. Acad. Sci. USA* **100**, 15924–15929 (2003).
6. Dressel, U. *et al.* The peroxisome proliferator-activated receptor β/δ agonist, GW501516, regulates the expression of genes involved in lipid catabolism and energy uncoupling in skeletal muscle cells. *Mol. Endocrinol.* **17**, 2477–2493 (2003).
7. Gilde, A.J. *et al.* Peroxisome proliferator-activated receptor (PPAR) α and PPARβ/δ, but not PPARγ, modulate the expression of genes involved in cardiac lipid metabolism. *Circ. Res.* **92**, 518–524 (2003).
8. Cheng, L. *et al.* Peroxisome proliferator-activated receptor δ activates fatty acid oxidation in cultured neonatal and adult cardiomyocytes. *Biochem. Biophys. Res. Commun.* **313**, 277–286 (2004).
9. Barak, Y. *et al.* Effects of peroxisome proliferator-activated receptor δ on placentation, adiposity, and colorectal cancer. *Proc. Natl. Acad. Sci. USA* **99**, 303–308 (2002).
10. Peters, J.M. *et al.* Growth, adipose, brain, and skin alterations resulting from targeted disruption of the mouse peroxisome proliferator-activated receptor β(δ). *Mol. Cell Biol.* **20**, 5119–5128 (2000).
11. Agah, R. *et al.* Gene recombination in postmitotic cells. Targeted expression of Cre recombinase provokes cardiac-restricted, site-specific rearrangement in adult ventricular muscle *in vivo*. *J. Clin. Invest.* **100**, 169–179 (1997).
12. Gutstein, D.E. *et al.* Conduction slowing and sudden arrhythmic death in mice with cardiac-restricted inactivation of connexin43. *Circ. Res.* **88**, 333–339 (2001).
13. Watanabe, K. *et al.* Constitutive regulation of cardiac fatty acid metabolism through peroxisome proliferator-activated receptor α associated with age-dependent cardiac toxicity. *J. Biol. Chem.* **275**, 22293–22299 (2000).
14. Kersten, S. *et al.* Peroxisome proliferator-activated receptor α mediates the adaptive response to fasting. *J. Clin. Invest.* **103**, 1489–1498 (1999).
15. Lee, Y. *et al.* Increased lipogenic capacity of the islets of obese rats: a role in the pathogenesis of NIDDM. *Diabetes* **46**, 408–413 (1997).
16. Chiu, H.C. *et al.* A novel mouse model of lipotoxic cardiomyopathy. *J. Clin. Invest.* **107**, 813–822 (2001).
17. Yagyu, H. *et al.* Lipoprotein lipase (LpL) on the surface of cardiomyocytes increases lipid uptake and produces a cardiomyopathy. *J. Clin. Invest.* **111**, 419–426 (2003).
18. Zhou, Y.T. *et al.* Lipotoxic heart disease in obese rats: implications for human obesity. *Proc. Natl. Acad. Sci. USA* **97**, 1784–1789 (2000).
19. Regan, T.J. & Weisse, A.B. Diabetic cardiomyopathy. *J. Am. Coll. Cardiol.* **19**, 1165–1166 (1992).
20. Zoneraich, S. & Mollura, J.L. Diabetes and the heart: state of the art in the 1990s. *Can. J. Cardiol.* **9**, 293–299 (1993).
21. Szczepaniak, L.S. *et al.* Measurement of intracellular triglyceride stores by H spectroscopy: validation *in vivo*. *Am. J. Physiol.* **276**, E977–E989 (1999).
22. Chatham, J.C., Gao, Z.P. & Forder, J.R. Impact of 1 wk of diabetes on the regulation of myocardial carbohydrate and fatty acid oxidation. *Am. J. Physiol.* **277**, E342–E351 (1999).
23. Shindo, Y., Osumi, T. & Hashimoto, T. Effects of administration of di-(2-ethylhexyl)phthalate on rat liver mitochondria. *Biochem. Pharmacol.* **27**, 2683–2688 (1978).
24. King, M.T. & Reiss, P.D. Separation and measurement of short-chain coenzyme-A compounds in rat liver by reversed-phase high-performance liquid chromatography. *Anal. Biochem.* **146**, 173–179 (1985).
25. Saddik, M., Gamble, J., Witters, L.A. & Lopaschuk, G.D. Acetyl-CoA carboxylase regulation of fatty acid oxidation in the heart. *J. Biol. Chem.* **268**, 25836–25845 (1993).
26. Coven, D.L. *et al.* Physiological role of AMP-activated protein kinase in the heart: graded activation during exercise. *Am. J. Physiol. Endocrinol. Metab.* **285**, E629–E636 (2003).